



Organic–inorganic hybrid proton exchange membrane based on polyhedral oligomeric silsesquioxanes and sulfonated polyimides containing benzimidazole



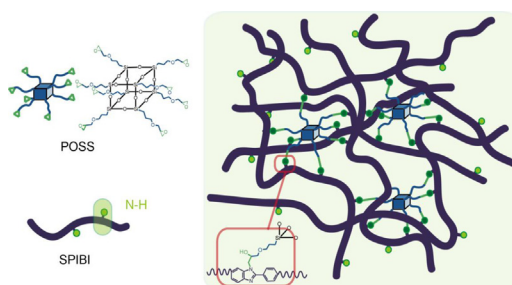
Haiyan Pan*, Yuanyuan Zhang, Hongting Pu, Zhihong Chang

Institute of Functional Polymers, School of Materials Science & Engineering, Tongji University, Shanghai 201804, China

HIGHLIGHTS

- Sulfonated polyimides containing benzimidazole group (SPIBI) are synthesized.
- The cross-linked membranes are prepared by SPIBI and glycidyl ether POSS.
- The cross-linked membranes exhibit improved hydrolytic and oxidative stability.
- The cross-linked membranes show improved mechanical property.

GRAPHICAL ABSTRACT



ARTICLE INFO

Article history:

Received 24 December 2013

Received in revised form

26 March 2014

Accepted 12 April 2014

Available online 24 April 2014

Keywords:

Proton exchange membrane

Sulfonated polyimide

Benzimidazole

Cross-linked

Glycidyl ether of polyhedral oligomeric silsesquioxanes

ABSTRACT

A new series of organic–inorganic hybrid proton exchange membranes (PEMs) were prepared using sulfonated polyimides containing benzimidazole (SPIBIs) and glycidyl ether of polyhedral oligomeric silsesquioxanes (G-POSS). SPIBIs were synthesized using 1,4,5,8-naphthalenetetracarboxylic dianhydride (NTDA), 5-amino-2-(4-aminophenyl) benzimidazole (APBIA) and 4,4'-diaminodiphenyl ether-2,2'-disulfonic acid (ODADS). The organic–inorganic cross-linked membranes can be prepared by SPIBIs with G-POSS by a thermal treatment process. The cross-linking density of the membranes was evaluated by gel fractions. The water uptake, swelling ratio, mechanical property, thermal behavior, proton conductivity, oxidative and hydrolytic stability of the cross-linked organic–inorganic membranes were intensively investigated. All the cross-linked membranes exhibit high cross-linking density for the gel fraction higher than 70%. Compared to pristine membranes (SPIBIs) and membranes without benzimidazole groups (SPI), the anti-free-radical oxidative and hydrolytic stabilities of cross-linked membranes are significantly higher. The anti-free-oxidative stability of SPIBI-100-P (cross-linked SPIBI membrane with 100% degree of sulfonation) is nearly four-fold higher than that of SPIBI-100. The proton conductivity of the cross-linked membranes ranges from 10^{-3} S cm^{-1} to 10^{-2} S cm^{-1} depending both on the degree of sulfonation (DS) of the SPIBI and temperature.

© 2014 Elsevier B.V. All rights reserved.

1. Introduction

Energy crisis and environmental pollution are the most severe challenges faced by the current generation. Fuel cells (FCs) have

attracted considerable research interest because of their high efficiency and environment friendliness [1–3]. As one of the key components of the proton exchange membrane FCs (PEMFCs), proton exchange membranes (PEMs) serve two functions: to transfer protons and separate the fuel and comburent. Preferred PEMs have high proton conductivity and low methanol

* Corresponding author. Tel.: +86 21 69580147.

E-mail address: phy@tongji.edu.cn (H. Pan).

permeability along with high chemical, thermal, and mechanical stability [4]. In the past few decades, several types of PEMs have been synthesized and investigated for application in FCs. Perfluorosulfonic acid membranes, such as Nafion[®], are predominantly used in practical and scientific systems. However, these membranes are expensive, have poor dimensional stability, and low mechanical property at high temperature and high humidity [5–7]. As alternatives to the perfluorinated polymers, various inexpensive sulfonated aromatic hydrocarbon polymers with excellent comprehensive properties have been developed [8–11]. Among these, sulfonated polyimides (SPIs) have attracted much attention for their potential use as the PEM of FCs [12–15].

Aromatic polyimides are a class of high performance engineering plastics with high tensile strength, unique thermal stability, excellent chemical resistance, and so on [16,17]. However, SPIs used in FCs have poor hydrolytic stability due to decomposition of the susceptible imide ($-\text{OC}-\text{N}-\text{CO}-$) groups in the polymer backbone. Although better than five-membered ring SPIs, six-membered ring SPIs also suffer from low hydrolytic stability [18–20]. Polybenzimidazole (PBI), with high heat resistance, excellent mechanical property, and anti-free-radical oxidative stability, shows great potential for use in the PEMFCs under high temperature and low humidity conditions. However, practical applications of PBI are restricted due to limitations. First, the solubility of PBI in most solvents at low temperature is poor, and second, the proton conductivity of PBI (sulfonated PBI or PBI doped with acid) is low [21–24]. Therefore, we introduced benzimidazole groups into the main chain of SPI in order to combine the advantageous properties and overcome the drawbacks of both SPI and PBI. One effective method to enhance the hydrolytic stability of SPI is cross-linking. Polyhedral oligomeric silsesquioxanes (POSS) have well-defined nanosized Si–O cage structures which make them a versatile additive for imparting enhanced mechanical property, thermal stability, oxidative resistance, and abrasion resistance [25–27]. POSS-based PEMs can improve the dimensional and hydrolytic stabilities as well as water retaining property [28]. Therefore, we selected the glycidyl ether of POSS (G-POSS) as the cross-linker to prepare cross-linked organic–inorganic hybrid PEMs. G-POSS has eight epoxy groups that can react with benzimidazoles and enhance cross-linking density.

In this study, we report the synthesis of SPIs containing benzimidazole groups (SPIBIs) by direct copolymerization. By changing the feed ratio of sulfonated and non-sulfonated diamines, a series of SPIBIs with different levels of sulfonation were synthesized successfully. A new type of SPIBI/POSS-based PEM was prepared by the solution casting method and *in-situ* cross-linking. Benzimidazoles in SPIBI react with the epoxy groups in G-POSS and form a polymer network within the membranes. The mechanical property, proton conductivity, and oxidative and hydrolytic stability of these membranes were also investigated.

2. Experimental

2.1. Materials

G-POSS was purchased from Hybrid Plastic. 4,4'-diaminodiphenyl ether (ODA) was purchased from Sinopharm Chemical Reagent Co. and recrystallized from ethanol. 1,4,5,8-naphthalenetetracarboxylic dianhydride (NTDA) was purchased from Alfa Aesar Co. 5-Amino-2-(4-aminophenyl) benzimidazole (APBIA) was purchased from Zhejiang Dragon Chemical Group Co. Triethylamine (Et_3N), methanol (AR grade), dimethyl sulfoxide (DMSO, analytical reagent grade), benzoic acid (CR grade), and acetone were supplied by Shanghai Chemical Reagent Co. *m*-cresol was distilled under reduced pressure and 4,4'-diaminodiphenyl

ether-2,2'-disulfonic acid was synthesized according to a procedure reported in literature [29].

2.2. Synthesis of sulfonated polyimide

A typical synthesis of SPIBI is described below using monomers NTDA/ODADS/APBIA (6/3/3, mol/mol). ODADS (3.0 mmol), *m*-cresol (24 mL), and Et_3N (1.0 mL) were added to a dry 100 mL three-necked flask under a flow of nitrogen gas. The mixture was mechanically stirred to dissolve ODADS; next, APBIA (3.0 mmol), NTDA (6.0 mmol), and benzoic acid were added. The mixture was stirred at room temperature for a few minutes and then heated sequentially at 80 °C for 4 h and 180 °C for 20 h. The viscous solution was diluted with *m*-cresol (10 mL), and the reaction was continued for additional 3–5 h. After cooling to 100 °C, additional *m*-cresol (10 mL) was added to further dilute the highly viscous solution and poured into acetone (200 mL). The fiber-like precipitate was filtered, washed with acetone in a Soxhlet extractor (to ensure the complete removal of solvent), and dried in vacuum at 60 °C for 24 h. The obtained SPIBI was designated as SPIBI-X, where X represents the expected degree of sulfonation (DS) of the polymers. The synthetic scheme and chemical structure of the SPIBI are shown in Fig. 1.

2.3. Film formation and proton exchange

The SPIBI (in Et_3N salt form) was dissolved in DMSO (5wt%). The solution was cast on clean glass plates and allowed to stand at 80 °C for 24 h in the vacuum. As an example, the process of the cross-linking membrane SPIBI-100 is described below. G-POSS (0.071 g) was added to a solution of SPIBI-100 (0.6 g) dissolved in DMSO (12 mL), and the solution was stirred at room temperature until it was homogenous. The solution was cast on the glass plate, heated at 80 °C for 6 h to evaporate the solvent, and then heated at 150 °C for 10 h to promote the reaction between epoxy and benzimidazole groups. Subsequently, the plate was immersed in deionized water until the membrane fell off naturally. Then the as-cast films were soaked in 1 mol L⁻¹ HCl solution at room temperature for 24 h. These membranes were thoroughly washed with deionized water and then dried in vacuum at 150 °C for 24 h. The thickness of each film was 40–50 μm.

The cross-linking membranes were denoted as SPIBI-X-P, where P represents the cross-linking of the membrane. The G-POSS feed content in SPIBI-X-P was a fixed value based on the content of benzimidazole groups.

2.4. Characterization of the membranes

2.4.1. ¹H NMR and Fourier-transform infrared (FTIR) spectra

¹H NMR spectrum of the polymer in deuterated dimethyl sulfoxide ($\text{DMSO}-d_6$) was acquired using a Varian Bruker AC-250 instrument. FTIR spectra of the membranes in KBr pellets were recorded using a Thermo Bruker Equinox/Hyperion 2000 spectrometer.

2.4.2. Viscosity

The viscosity of SPIBI (in Et_3N salt form) was measured in concentrated sulfuric acid (95%) at 25 °C using a Ubbelohde viscometer, and the intrinsic viscosity $[\eta]$ was calculated by extrapolation using the Huggins and Kraemer equations.

2.4.3. Gel fraction

The degree of membrane cross-linking was characterized by the gel fraction. The gel fraction was measured by solvent extraction [30].

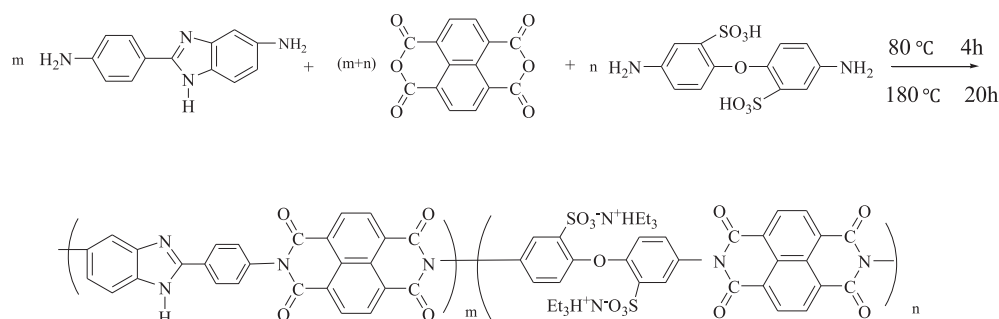


Fig. 1. Synthetic procedure of the sulfonated polyimide containing benzimidazole.

Sample (0.1–0.3 g) was placed in DMSO and extracted using a Soxhlet extractor until no further soluble polymer was observed. The remaining sample was dried to a constant mass. The gel fraction, W_{gel} , of the membrane was calculated using Eq. (1),

$$W_{\text{gel}} = \frac{W_1}{W_0} \times 100\% \quad (1)$$

where W_0 is the original mass of the dry membrane and W_1 is the mass of the dry membrane after extraction.

2.4.4. Ion exchange capacity (IEC)

The theoretical IEC was calculated from the initial molar composition of the sulfonic groups in the entire polymer molecule. Experimental IEC was measured by titration. The membranes were soaked in saturated NaCl for 24 h. The protons released due to the exchange with Na^+ ions were titrated against 0.1 mol L^{-1} NaOH and monitored using phenolphthalein as the indicator. The experimental IEC was determined using Eq. (2),

$$\text{IEC} = \frac{V_{\text{NaOH}} \times M_{\text{NaOH}}}{W} \quad (2)$$

where V_{NaOH} is the volume of NaOH consumed and M_{NaOH} is the normality of NaOH.

2.4.5. Thermal stability of the membranes

Thermogravimetric analysis (TGA) of the membranes was performed using a STA 449C (Netzsch Co.) in the temperature range 30–700 °C with a heating rate of $10 \text{ }^\circ\text{C min}^{-1}$ under nitrogen atmosphere.

2.4.6. Tensile properties

Tensile properties of the membrane were evaluated at room temperature, 50% relative humidity (RH), and a strain speed of 50 mm min^{-1} using a universal material testing machine (DXLL-5000) according to ASTM D882-02.

2.4.7. Water uptake and swelling ratio of the membranes

The water uptake of the membranes were measured after immersing three pre-weighed sheets of membranes (20–30 mg per sheet, dried under vacuum at 100 °C for 2 days prior to weighing) into water at 25 °C or 80 °C for 48 h. Subsequently, the membranes were taken out, wiped with tissue paper, and immediately weighed on a microbalance. The water uptake (WU) of the membranes was calculated using Eq. (3) [4],

$$\text{WU} = \frac{W_{\text{wet}} - W_{\text{dry}}}{W_{\text{dry}}} \times 100\% \quad (3)$$

where W_{dry} and W_{wet} are the weight of the corresponding dry and wet membrane sheets, respectively. The reported values for water uptake of the membrane are an average of at least three independent measurements.

Similar to the water uptake measurements, the measurement of the swelling ratio of the membrane was carried out after immersing three sheets of membranes (20–30 mg per sheet) into water at 25 or 80 °C for 5 h. The membrane was removed, and the length of the swollen membrane was measured using a Vernier caliper. The swelling ratio (SR) of the membrane can be calculated using Eq. (4) [17],

$$\text{SR} = \frac{L_{\text{wet}} - L_{\text{dry}}}{L_{\text{dry}}} \times 100\% \quad (4)$$

where L_{dry} and L_{wet} are the lengths of dry and swollen membranes, respectively. The reported values of swelling ratios of the membrane are an average of at least three independent measurements.

2.4.8. Proton conductivity of the membrane

The proton conductivity of the membranes was measured using Electrochemical Impedance Lab CHI 604B (CH Instruments Inc.), which worked in the galvanostatic mode and produced a proton current across the membrane. The test frequency was in the range 1–10,000 Hz. The test cell was placed in a thermo-controlled water bath for measurement at a RH of 100%. The in-plane impedance of the membrane was measured from 40 °C to 105 °C [4]. The proton conductivity of the membranes was measured at different temperatures. The proton conductivity σ can be determined using Eq. (5),

$$\sigma = \frac{d}{SR} \quad (5)$$

where d is the distance between the two electrodes, S is the sectional area of the membrane, and R is the measured impedance of the membrane.

2.4.9. Membrane stability

The hydrolytic stability of the membranes toward moisture was evaluated by soaking the membranes in deionized water at 80 °C and observing the loss of mechanical property in the hydrated membranes. The criterion for the judgment of the loss of mechanical property was the breaking of membrane on gentle bending [30].

The oxidative stability of the membranes was examined after immersing the membranes in Fenton's reagent (3 ppm FeSO_4 in 3% H_2O_2) at 80 °C. Oxidative stability of the membranes was characterized by the time immersed membrane to become brittle (i.e., membrane broke when bent gently).

3. Results and discussion

3.1. Synthesis of the benzimidazole-containing sulfonated polyimide

SPIBIs are synthesized by the co-polymerization of ODADS, APBIA, and NTDA monomers (Fig. 1). By changing the ODADS-to-APBIA molar ratio, a series of SPIBIs with different degrees of sulfonation (DS) are obtained. The SPIBI is designated as SPIBI-X, where X (in %) represents the expected DS. DS is calculated from the ODADS-to-APBIA feed ratios, which are listed in Table 1. The intrinsic viscosity ($[\eta]$) of SPIBI varies between 0.44 dL g^{-1} and 1.99 dL g^{-1} and increases with the increasing DS (Table 1). This results from the increase in the interaction between the main chains of polymers due to increased hydrogen bonding interactions between sulfonic acid and benzimidazole groups. The membranes cast from the DMSO solutions are tough and flexible, as demonstrated by their ability to fold a couple of times without breaking down.

Fig. 2 shows the FTIR spectra of the SPIBI-80, SPIBI-100 and SPIBI-120. Strong absorption bands around 1711 cm^{-1} and 1668 cm^{-1} are assigned to the stretching vibrations of carbonyl groups in the imido rings. The C–N–C stretching vibrations of the imide ring are observed around 1343 cm^{-1} . The bands around 1081 cm^{-1} and 1022 cm^{-1} represent the stretching vibrations of sulfonic acid group. The absorption bands at 1081 cm^{-1} and 1022 cm^{-1} become stronger with increasing DS. These observations confirm that sulfonic acid group has been incorporated to the main chain of the polymer. The IR absorption band of the sulfonic acid is shifted from 1088 cm^{-1} in SPI to 1081 cm^{-1} in SPIBI, indicating the hydrogen bonding interaction between sulfonic acid and benzimidazole groups [29,31,32].

Fig. 3 shows the ^1H NMR spectrum of SPIBI-100. The peak at $\delta 13.3 \text{ ppm}$ is attributed to the acidic proton of benzimidazole. The signals for H_1 and H_6 are observed at $\delta 8.2$ – 9.0 ppm . The chemical shifts of signals for H_2 , H_3 , H_4 , H_5 , H_7 , H_8 , and H_9 appear at $\delta 6.5$ – 8.0 ppm . The ratio of integration for the peaks in the $\delta 8.2$ – 9.0 ppm and $\delta 6.5$ – 8.0 ppm regions is 9:12, indicating that the feed ratio of the NTDA/ODADS/APBIA is equal to 2:1:1. Therefore, it can be concluded that benzimidazole groups are successfully imported into SPIBI.

3.2. Membrane preparation and cross-linking

During the preparation of membranes, the nucleophilic benzimidazole in SPIBI reacts with the epoxy group of G-POSS (Fig. 4). The functional groups in SPIBI-100, SPIBI-80-P, SPIBI-100-P, SPIBI-120-P, and G-POSS are characterized by FTIR (Fig. 5). The strong signal observed at 910 cm^{-1} in the spectrum of G-POSS is assigned to the vibrations of the epoxy group. The strong absorption peak corresponding to epoxy groups is absent in the FTIR spectrum of SPIBI-X-P, providing the evidence for the reaction between epoxy and benzimidazole groups.

The gel fraction of the cross-linked membranes indirectly assesses the degree of cross-linking. SPIBI has a good solubility in DMSO, while cross-linked SPIBI-X-P is not soluble in it. Therefore, DMSO is selected as the solvent to evaluate gel fraction. The

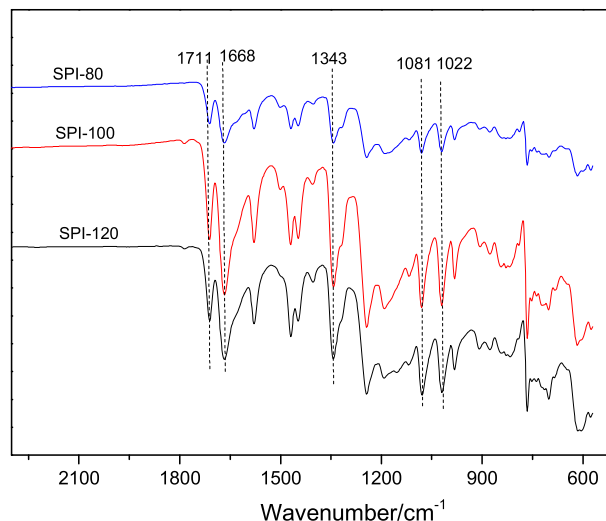


Fig. 2. The FTIR spectrum of the SPIBI.

measured gel fractions of the cross-linked membranes are listed in Table 2. The gel fraction of the cross-linked membrane is higher than 70%. This proves that the benzimidazoles in SPIBI react with the epoxy groups of the G-POSS during cross-linking. The gel fraction of SPIBI-X-P is directly proportional to the content of the benzimidazole in SPIBI. With increasing value of X, the content of the benzimidazole decreases, resulting in fewer cross-linking points and lower degree of the cross-linking.

3.3. Thermal stability

TGA is used to characterize the thermal stabilities of pure and cross-linked membranes. Fig. 6 shows the typical TGA curves for SPIBI-X and SPIBI-X-P. Two weight-loss stages are observed for SPIBI. The first weight-loss indicated above 380°C is attributed to the decomposition of sulfonic acid groups. The second weight loss over 560°C indicates the degradation of the polyimide backbone. The cross-linked membranes (SPIBI-X-P) also exhibit a two-step degradation pattern, similar to that of SPIBI. The first weight-loss in cross-linked membranes occurs in the temperature range 327 – 354°C . This is attributed to the degradation of the sulfonic acid group and C–H bond of the aliphatic chain in G-POSS. This temperature range is a little lower than that pure SPIBI-X for the low degradation temperature of the aliphatic C–H in G-POSS. The second weight loss in cross-linked membranes occurs at 564 – 576°C , indicating the degradation of the backbone chains in SPIBI-X and G-POSS. All the SPIBIs and cross-linked membranes show excellent thermal stability higher than 320°C , indicating their prospective application in high-temperature FCs.

3.4. Ion exchange capacity, water uptake and swelling ratio

As shown in Table 3, the experimentally determined IECs are much lower than the theoretical values, which can be due to two reasons: 1) incomplete proton exchange in the experiment; and 2) H-bond interactions between imidazole group of the benzimidazole in the SPIBI and the sulfonic acid can preclude the proton from being exchanged. The IEC depends on the molar ratio of the sulfonic acid in the polymer chain and the molecular weight of the repeating unit. With increasing DS, the value of IEC increases.

Since PEMs in FCs are currently operated around 80°C , the water uptake and swelling ratio of the SPIBI-X and SPIBI-X-P are measured at both room temperature (25°C) and 80°C . The results

Table 1
The feed ratio and the intrinsic viscosity of SPIBI.

Polymers	ODADS/mmol	APBIA/mmol	NTDA/mmol	DS/%	$[\eta]/(\text{dL g}^{-1})$
SPI-80	4	6	10	80	0.44
SPI-100	5	5	10	100	1.34
SPI-120	6	4	10	120	1.99

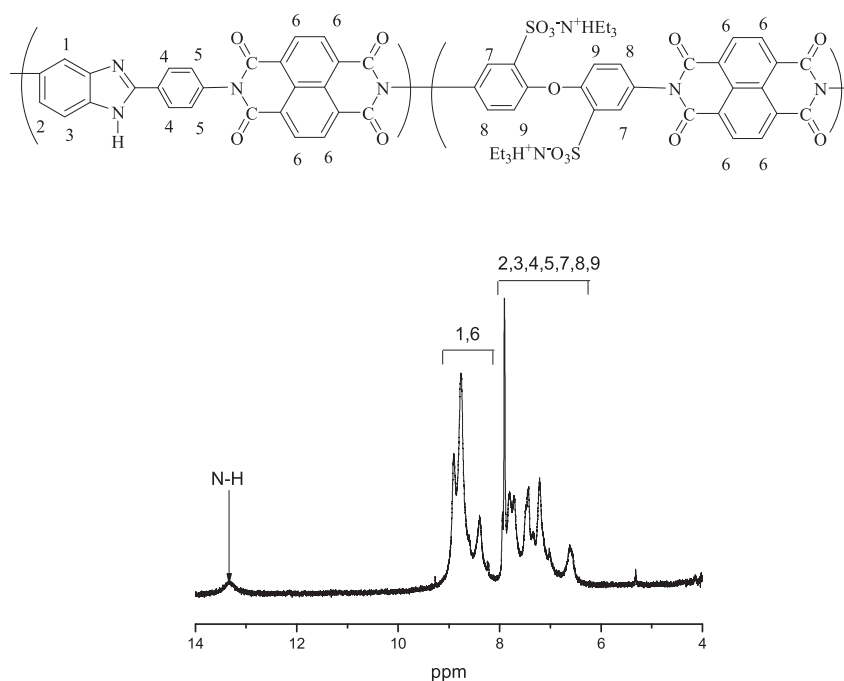


Fig. 3. The ^1H NMR spectra of the SPIBI-100 in $\text{DMSO}-d_6$.

are shown in Table 3. The hydrolytic stability of SPIBI-80 is poor, it breaks after being in the water at 80°C for 48 h. Therefore, no water uptake and swelling ratio data of SPIBI-80 at 80°C can be determined. The water uptake of the SPIBI-X and SPIBI-X-P increase with the IEC and temperature (Table 3). Compared to SPIBI-X, the cross-linked membranes exhibit lower water uptake. This is attributed to the lower IEC and cross-linking, both of which restrict the degree of mobility of the hydrophilic sulfonic acid groups. The swelling ratio of the membrane is an important property for PEMs because an excessively high swelling ratio can destroy the membrane-electrode-assembly (MEA) in PEMFCs. A high swelling ratio is associated with low dimensional stability. As evident from Table 3, the swelling ratio increases with increasing temperature, and this is similar to that of water uptake. The swelling ratio of the cross-linked membrane is much lower than that of SPIBI-X membranes at both temperatures. At room temperature, even with a similar

water uptake, SPIBI-X-P has a significantly lower swelling ratio than that of the SPIBI-X. This can be attributed to cross-linking in SPIBI-X-P, which restrains its swelling. The swelling ratio of the cross-linked membrane decreases from 6.0% (pure SPIBI-120) to 1.8–4.1% at 80°C . These data indicate that the SPIBI-X-Ps have much better dimensional stabilities than those of SPIBI-Xs.

3.5. Tensile property

Adequate mechanical strength is crucial in the preparation of MEA and endurance of PEM in FCs. The tensile strength is used to characterize the mechanical strength of SPIBI-X and SPIBI-X-P.

The tensile strength of SPIBI-X increases with increasing DS due to the increase in the molecular weight of SPIBI-X (Fig. 7). Compared to pure SPIBI-X, the cross-linked membranes exhibit higher tensile strength. This is attributed to the existence of the

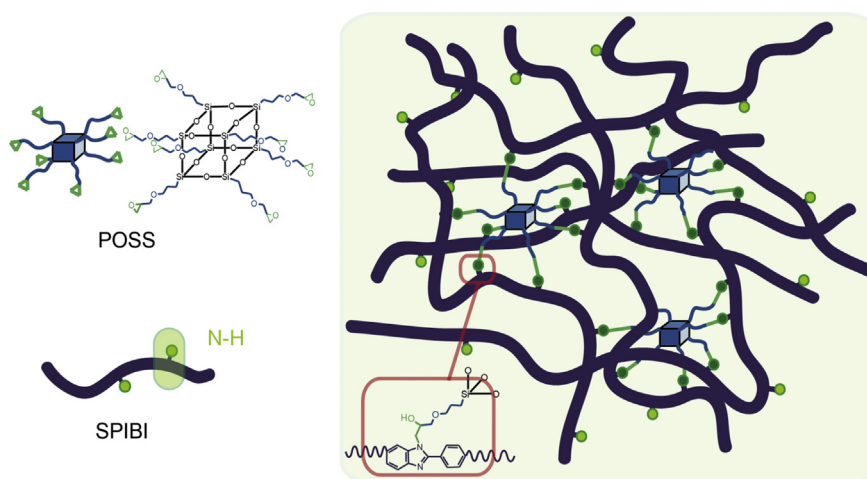


Fig. 4. The schematic representation of the cross-linked membranes.

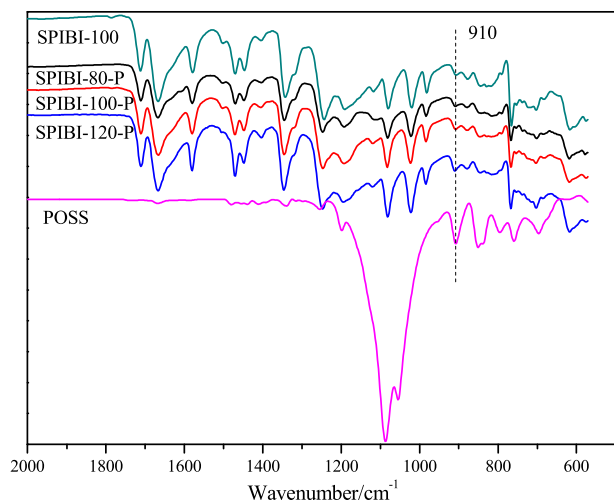


Fig. 5. The FTIR spectrum of the SPIBI-80, SPIBI-X-P and G-POSS.

cross-linked network within SPIBI-X-P membranes. The increase in tensile strengths between SPIBI-X and SPIBI-X-P are 24.9%, 25.3%, and 13.3% when X is 80, 100 and 120, respectively. The reasons are: 1) the higher cross-linking density is, the higher increasing amplitude is; 2) large cage structure of the POSS increases the rigidity of the main chain and weakens the interaction between the molecular chains, which decreases the tensile strength. Based on these two factors, the amplitude of tensile strength first increases and then decreases. The tensile strength of the as-synthesized organic–inorganic hybrid PEMs (54.6 MPa–101.9 MPa) is much higher than that of Nafion[®]212 (26.6 MPa) [33], indicating that they meet the mechanical requirements of a PEM in FCs.

3.6. Proton conductivity

All the membranes were hydrated by soaking in water for over 24 h before the proton conductivities were measured. The results are shown in Fig. 8. All the membranes show an increase in the proton conductivity with increasing temperature. Compared to the conductivity of pure SPIBI-Xs, SPIBI-X-Ps exhibit both lower and higher proton conductivities. The proton conductivity of the G-POSS-based cross-linked membranes is affected by three factors: 1) G-POSS in the cross-linked membrane has no proton conductivity and the total number of sulfonic groups in the cross-linked membrane decreases. Lower content of sulfonic acids reduced proton conductivity. 2) The amount of water retained by the membrane (G-POSS, due to its cage structure, has excellent water retention property). Increased water content leads to increase in proton conductivity. 3) the number of free imidazole groups, i.e., the molecules that have not participated in the reaction with the epoxy groups in G-POSS. Presence of free imidazoles, with their ability to conduct protons, increases proton conductivity. The proton conductivity of SPIBI-X-P with a lower value for X is higher than that of the SPIBI-X with the same DS. This can be attributed to the presence of high content of G-POSS and imidazole groups in SPIBI-X-P.

Table 2
The gel fraction of the SPIBI-X-P.

Membranes	Thickness/ μm	Content of POSS/wt%	Gel fraction/%
SPIBI-80-P	53	14.8	90.1
SPIBI-100-P	46	11.8	89.9
SPIBI-120-P	52	9.4	72.9

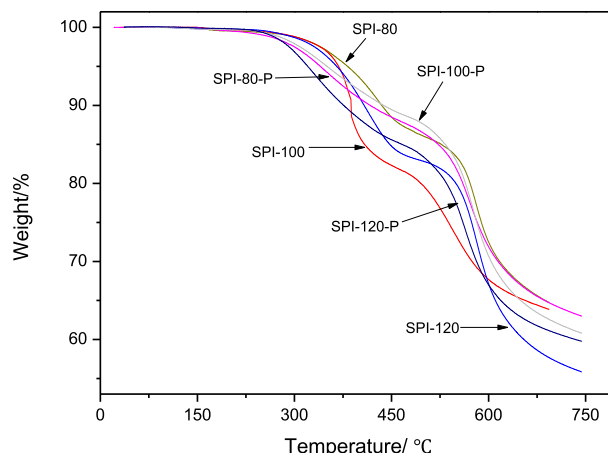


Fig. 6. The TG curves of the SPIBI-X and SPIBI-X-P, nitrogen atmosphere, heating rate $10\text{ }^{\circ}\text{C min}^{-1}$.

However, all the membranes have considerably high proton conductivity ranging from $3.2 \times 10^{-3}\text{ S cm}^{-1}$ to $1.3 \times 10^{-2}\text{ S cm}^{-1}$ (in the temperature range $40\text{--}105\text{ }^{\circ}\text{C}$).

The values of the activation energy E_a , for proton conduction by each cross-linked membranes are calculated using the Arrhenius equation (6),

$$\sigma = \sigma_0 \exp\left(-\frac{E_a}{RT}\right) \quad (6)$$

where R is the Boltzmann's constant, E_a is the activation energy, and T is the temperature. The calculated E_a for proton conduction in the cross-linked membranes is $13.9\text{--}17.3\text{ kJ mol}^{-1}$. These results indicate that the proton transport in the cross-linked membranes is predominantly via the vehicle mechanism [34]. The Vehicle mechanism suggests that the proton transport is controlled through H_3O^+ and H_5O_2^+ mediated proton transfer.

3.7. Membrane stability

The hydrolytic and oxidative stability of the proton exchange membrane is of great importance to the lifetime and performance of the PEMFC. The data is shown in Table 4. For comparison, the membrane from NTDA/ODADS/ODA (SPI-100) is prepared and tested for its hydrolytic and oxidative stability.

In general, the membrane with lower IEC and water uptake has a higher hydrolytic stability. As shown in Table 4, although SPIBI-80 has the lowest IEC and water uptake, the hydrolytic stability of the SPIBI-80 is so poor that it only maintains its mechanical stability only for 27 h. This is because the molecular weight of the SPIBI-80 is low. SPIBI-100 exhibits excellent hydrolytic stability (1120 h), which is significantly better than that of SPI-100 (without

Table 3
The ion exchange capacity, water uptake and swelling ratio of the SPIBI-X and SPIBI-X-P.

Membranes	Water uptake/%		Swelling ratio/%		IEC/(mmol g ⁻¹)	
	25 $^{\circ}\text{C}$	80 $^{\circ}\text{C}$	25 $^{\circ}\text{C}$	80 $^{\circ}\text{C}$	Theoretical	Measured
SPI-80	16.4	Broken	3.7	Broken	1.56(0.39)	0.50
SPI-80-P	13.3	16.7	2.6	2.7	—	0.24
SPI-100	27.3	76.3	4.8	5.1	1.90(0.95)	0.74
SPI-100-P	24.5	40.6	1.0	1.8	—	0.35
SPI-120	44.7	91.3	5.3	6.0	2.22(1.48)	1.20
SPI-120-P	38.1	64.6	3.6	4.1	—	0.82

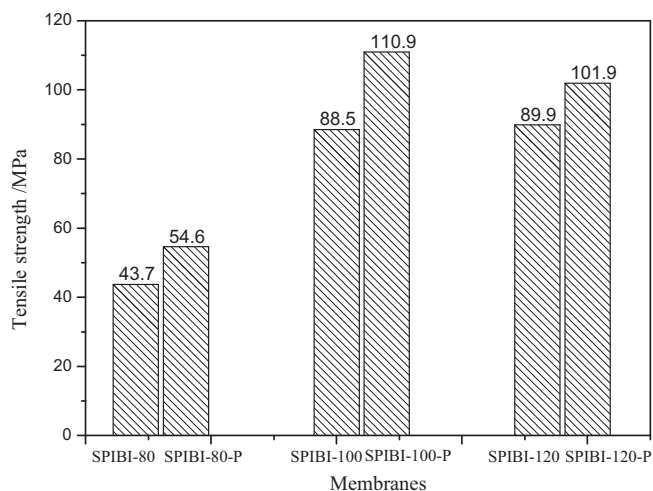


Fig. 7. The tensile strength of the SPIBI-X and SPIBI-X-P.

the benzimidazole group). This can be attributed to the ionic cross-linking of benzimidazole and sulfonic acid groups. Compared to pure SPIBI-X, all the cross-linked membranes show higher hydrolytic stabilities. SPIBI-80-P maintains its integrity after being soaked in the water at 80 °C for more than 1,440 h, which is much longer than that for SPIBI-80 (27 h). This hydrolytic stability results from the cross-linking within SPIBI-X-P, which retards chain scission. All the cross-linked membranes, except SPIBI-120-P, exhibit excellent hydrolytic stabilities (for >1440 h); higher than that for several ODADS-based SPIs [18,28].

The oxidative stability of the membrane is characterized by the accelerated test in Fenton's reagent at 80 °C. As expected, with the increase in DS, the resistance of the membrane towards oxidation decreases. SPIBI-120 membrane becomes brittle after being soaked in Fenton's reagent for 195 min, while SPIBI-80 becomes brittle after 360 min. Compared to SPI-100, SPIBI-100 shows better oxidative stability. The reason for this is the presence of benzimidazole groups, which can react with the free radicals. The oxidative stability of SPIBI-100-P is superior to that of SPIBI-X. SPIBI-100-P membrane becomes brittle after being soaked in Fenton's reagent for 1110 min, while SPIBI-100 exhibited oxidative stability for 220 min. SPIBI-100-P is nearly five-fold more stable toward oxidative degradation than the pure membrane. The

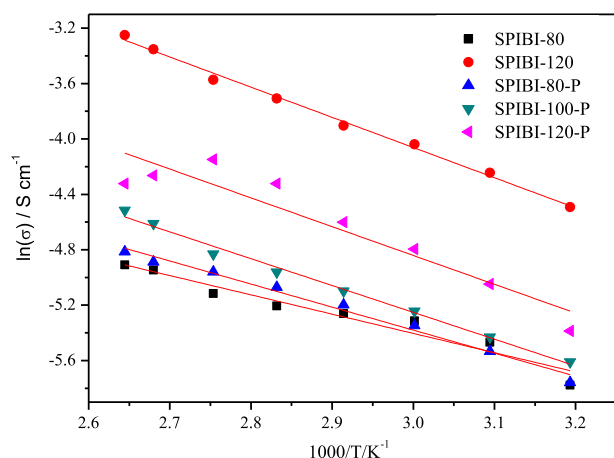


Fig. 8. The proton conductivity of the SPIBI-80, SPIBI-120 and SPIBI-X-P, 100% relative humidity.

Table 4

The hydrolysis and oxidative stability of the SPIBI-X and SPIBI-X-P.

Membranes	Thickness/ μm	HS/h	OS/min
SPI-100 ^a	50	42	165
SPIBI-80	56	27	360
SPIBI-80-P	53	>1440	605
SPIBI-100	56	1120	220
SPIBI-100-P	46	>1440	1110
SPIBI-120	50	140	195
SPIBI-120-P	52	338	220

^a Membrane of NTDA/ODADS/ODA.

reasons are as follows: 1) the cross-linked network within the SPIBI-X-P enhances the oxidative stability of the membrane; and 2) when the membrane is attacked by free radicals, the Si–O–Si bonds in POSS-based membranes are cleaved and leads to the formation of a layer of SiO₂ layer, which protect the membrane from further attack [35]. All the POSS-based cross-linked membranes exhibit better oxidative stability than SPIBI or SPI membranes.

4. Conclusions

In this study, SPIBIs are synthesized using NTDA, APBIA and ODADS as the monomers. By changing ODADS-to-APBIA molar ratio, a series of SPIBIs with different DS are obtained. During the membrane preparation, benzimidazoles in the obtained SPIBI react with the epoxy group of G-POSS to afford cross-linked organic–inorganic membranes. Compared to pure SPIBI, the cross-linked membranes exhibit highly improved dimensional stability, mechanical property, anti-free-oxidative and hydrolytic stability. The tensile strength of the cross-linked membranes ranges from 54.6 MPa to 101.9 MPa, which is significantly higher than that of pure membranes (43.7 MPa–89.9 MPa). With increasing DS, the dimensional stability of the cross-linked membranes decreases, whereas the proton conductivity increases. The cross-linked membranes show considerable proton conductivity in the range from $3.2 \times 10^{-3} \text{ S cm}^{-1}$ to $1.3 \times 10^{-2} \text{ S cm}^{-1}$, depending both on the DS in the SPIBI and temperature. The migration of protons in the cross-linked membranes can be explained by the vehicle mechanism. SPIBI-80-P maintains its integrity after being soaked in the water at 80 °C for more than 1,440 h, which is much longer than that for SPIBI-80 (27 h). SPIBI-100-P membrane becomes brittle after being soaked in Fenton's reagent for 1110 min, relative to 220 min for SPIBI-100. All cross-linked membranes show significantly superior anti-free-radical oxidative and hydrolytic stabilities than the pure SPIBI and SPI. In summary, the POSS-based cross-linked SPIBI membranes prove to be a promising material and a novel PEM and may have potential applications in FCs.

Acknowledgments

The project is sponsored by National Science Foundation of China (51303134, 51203119), Fundamental Research Funds for the Central Universities (0500219149), Research Fund for the Doctoral Program of Higher Education (20120072110062), China High-Tech Development 863 Program (SS2012AA110501).

References

- [1] M.A. Hickner, H. Ghassemi, Y.S. Kim, B. Einsla, J.E. McGrath, *Chem. Rev.* 104 (2004) 4587–4612.
- [2] T. Ous, C. Arcoumanis, *J. Power Sources* 240 (2013) 558–582.
- [3] B.C.H. Steele, A. Heinzel, *Nature* 414 (2001) 345–352.
- [4] H.Y. Pan, H.T. Pu, M. Jin, D.C. Wan, A.D. Modestov, *Electrochim. Acta* 89 (2013) 577–584.
- [5] D. Markova, A. Kumar, M. Klapper, K. Müllen, *Polymer* 50 (2009) 3411–3421.

- [6] H.T. Pu, D. Wang, *Electrochim. Acta* 51 (2006) 5612–5617.
- [7] K. Eom, Y.Y. Jo, E. Cho, T.H. Lim, J.H. Jang, H.J. Kim, B.K. Hong, J.H. Lee, *J. Power Sources* 198 (2012) 42–50.
- [8] H.W. Zhang, P.K. Shen, *Chem. Soc. Rev.* 41 (2012) 2382–2394.
- [9] A. Chandan, M. Hattenberger, A. El-kharouf, S.F. Du, A. Dhir, V. Self, B.G. Pollet, A. Ingram, W. Bujalski, *J. Power Sources* 231 (2013) 264–278.
- [10] J. Grodzinski, *Polym. Adv. Technol.* 18 (2007) 785–799.
- [11] V. Neburchilov, J. Martin, H.J. Wang, J.J. Zhang, *J. Power Sources* 169 (2007) 221–238.
- [12] E.A. Mistri, A.K. Mohanty, S. Banerjee, H. Komber, B. Voit, *J. Membr. Sci.* 441 (2013) 168–177.
- [13] H.Y. Pan, X.L. Zhu, X.G. Jian, *Electrochim. Acta* 55 (2010) 709–714.
- [14] T. Watari, J.H. Fang, K. Tanaka, H. Kita, K. Okamoto, T. Hirano, *J. Membr. Sci.* 230 (2004) 111–120.
- [15] M.R. Hibbs, C.J. Cornelius, *J. Mater. Sci.* 48 (2013) 1303–1309.
- [16] C.Y. Tseng, Y.S. Ye, J. Joseph, K.Y. Kao, J. Rick, S.L. Huang, B.J. Hwang, *J. Power Sources* 196 (2011) 3470–3478.
- [17] C. Lee, S. Sundar, J. Kwon, H. Han, *J. Polym. Sci. Part A Polym. Chem.* 42 (2004) 3612–3620.
- [18] X.L. Zhu, H.Y. Pan, Y.F. Liang, X.G. Jian, *Eur. Polym. J.* 44 (2008) 3782–3789.
- [19] T. Watari, H.Y. Wang, K. Kuwahara, K. Tanaka, H. Kita, K. Okamoto, *J. Membr. Sci.* 219 (2003) 137–147.
- [20] C. Genies, R. Mercier, B. Sillion, R. Petiaud, N. Cornet, G. Gebel, M. Pineri, *Polymer* 42 (2001) 5097–5105.
- [21] H.J. Xu, K.C. Chen, X.X. Guo, J.H. Fang, J. Yin, *Polymer* 48 (2007) 5556–5564.
- [22] E.V. Van, A. Chairuna, G. Merle, S.P. Benito, Z. Borneman, K. Nijmeijer, *J. Power Sources* 222 (2013) 202–209.
- [23] X.P. Li, C. Liu, G.P. Yu, X.G. Jian, *J. Membr. Sci.* 423–424 (2012) 128–135.
- [24] L.A. Diaz, G.C. Abuin, H.R. Corti, *J. Membr. Sci.* 411 (2012) 35–44.
- [25] J.W. Choi, R. Tamaki, S.G. Kim, R.M. Laine, *Chem. Mater.* 15 (2003) 3365–3375.
- [26] J.C. Huang, C.B. He, Y. Xiao, K. Mya, J. Dai, Y.P. Siow, *Polymer* 44 (2003) 4491–4499.
- [27] S. Subianto, M.K. Mistry, N.R. Choudhury, N.K. Dutta, R. Knott, *Appl. Mater. Interface* 1 (2009) 1173–1182.
- [28] Y.W. Chang, G. Shin, *J. Ind. Eng. Chem.* 17 (2011) 730–735.
- [29] J.H. Fang, X.X. Guo, S. Harada, T. Watari, K. Tanaka, H. Kita, K. Okamoto, *Macromolecules* 35 (2002) 9022–9028.
- [30] S. Xue, G.P. Yin, *Polymer* 47 (2006) 5044–5049.
- [31] X.L. Zhu, Y.F. Liang, H.Y. Pan, Y.X. Zhang, X.G. Jian, *J. Membr. Sci.* 31 (2008) 59–65.
- [32] R. Bouchet, E. Siebert, *Solid State Ionics* 118 (1999) 287–299.
- [33] F.Q. Liu, B.L. Yi, D.M. Xing, J.G. Yu, H.M. Zhang, *J. Membr. Sci.* 212 (2003) 213–223.
- [34] B. Smitha, S. Sridhar, A.A. Khan, *Macromolecules* 37 (2004) 2233–2239.
- [35] K. Yokota, S. Abe, M. Tagawa, M. Iwata, M. Iwata, J. Ishizawa, Y. Kimoto, R. Yokota, *Polymer* 22 (2010) 237–251.